Analytical Methods

Accepted Manuscript

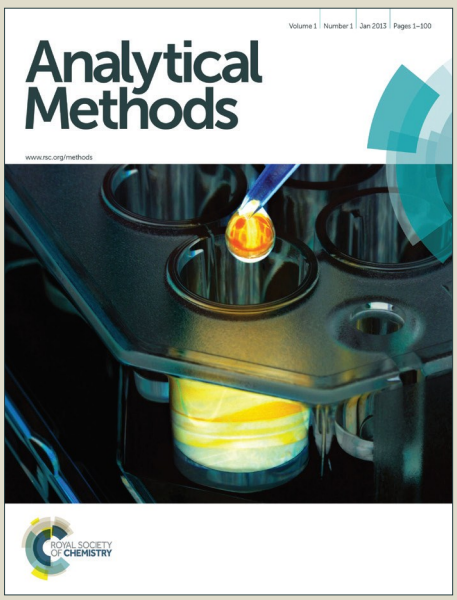

This is an *Accepted Manuscript*, which has been through the Royal Society of Chemistry peer review process and has been accepted for publication.

Accepted Manuscripts are published online shortly after acceptance, before technical editing, formatting and proof reading. Using this free service, authors can make their results available to the community, in citable form, before we publish the edited article. We will replace this *Accepted Manuscript* with the edited and formatted *Advance Article* as soon as it is available.

You can find more information about *Accepted Manuscripts* in the Information for Authors.

Please note that technical editing may introduce minor changes to the text and/or graphics, which may alter content. The journal's standard Terms & Conditions and the Ethical guidelines still apply. In no event shall the Royal Society of Chemistry be held responsible for any errors or omissions in this *Accepted Manuscript* or any consequences arising from the use of any information it contains.

ROYAL SOCIETY OF CHEMISTRY

www.rsc.org/methods

Analytical Methods

RSCPublishing

ARTICLE

A metal-enhanced fluorescence study of primary amines: determination of aminoglycosides with europium and gold nanoparticles

Cite this: DOI: 10.1039/x0xx00000x

Received 00th January 2012,
Accepted 00th January 2012

DOI: 10.1039/x0xx00000x

www.rsc.org/

Mehmet Gokhan Caglayan,[a] and Feyyaz Onur[a]

[a] Ankara University, Faculty of Pharmacy, Department of Analytical Chemistry, Ankara, Turkey

This paper describes a lipoic acid capped europium nanoparticle-based assay for the fluorimetric detection of primary amines. The assay is based on fluorescence quenching resulted from complex formation between amines and lipoic acid on the surface of europium nanoparticles. For application of the assay, the aminoglycosides were determined in pharmaceutical and milk. Determination of the aminoglycosides were conducted via fluorescence quenching at 315 nm (λ_{exc}=280 nm) at a pH of 5. The metal enhanced fluorescence method with gold nanoparticles was used, in order to enhance the fluorescence of europium nanoparticles. In this way, the detection limits of aminoglycosides were lowered. The Stern-Volmer constants and the ground-state UV spectra of interaction proved the static quenching that stemmed from the reaction between amines and lipoic acid. Three members of aminoglycosides; amikacin, gentamicin and tobramycin were quantified in the range of 0.75-27.5 μg.mL^{-1}, 0.40-26 μg.mL^{-1} and 0.20-25 μg.mL^{-1} respectively.

1. Introduction

Lanthanides have unique fluorescence characteristics; the emissions include 4f orbitals (forbidden transitions) and the weak absorptivity of lanthanides increased in presence of some organic ligands. Accordingly the fluorescence of lanthanides sensitive to the surrounding medium appear to be good sensors for the target molecules.[1]

Nanoparticle based spectroscopic assays have the capacity to improve the sensitivity and selectivity of spectroscopy.[2] Metal nanoparticles are of interest in diverse areas of science due to their outstanding optical, electrical, magnetic and catalytic features.[3] They greatly contribute to optical spectroscopy, including fluorescence spectroscopy, owing to their size-dependent and tunable optical properties. Thus, europium nanoparticles (EuNP) combine the unique fluorescence properties of lanthanides and the tunable and interesting features of metal nanoparticles.

Metal nanoparticles, especially gold and silver, can also be used in the enhancement of fluorescence signals (Metal Enhanced Fluorescence, MEF). Fluorescence enhancement is achieved through the interaction of their surface plasmon electrons with the fluorophore groups which causes an increase in the electric field around these groups. In this way, the selectivity of a method can be increased while detection limits can be decreased.[4]

Aminoglycosides a large group of antibiotics that have amino sugars glycosidically linked to aminocyclitols are administered in the treatment of gram-negative bacterial infections[5]. Although they are a therapeutically essential class of antibiotics, their usefulness is often restricted by their toxic potential and residues in animal originated foods.[6] Ototoxicity and nephrotoxicity are commonly reported adverse effects.[7] Consequently, a surveillance program of aminoglycosides residue has been implemented by public institutions to provide food safety and to prevent antibiotic resistance. However, the analysis of aminoglycosides is difficult due to the lack of chromophore groups and the low volatility. Another difficulty encountered in the analysis of aminoglycosides is its high polarity which hinders extraction and leads to weak retention in liquid chromatography.[8] Thus, the development of accurate and simple assays for aminoglycosides is of great concern for food safety programs and the pharmaceutical industry.

There are liquid chromatographic[9-10] capillary electrophoretic[11-12], voltammetric[13-14], spectrophotometric[15-16] and spectrofluorimetric[17-18] methods for the determination of

aminoglycosides, however there are not any metal enhanced fluorescence assay for these amine containing antibiotics.

In this study, we developed a europium nanoparticles based fluorimetric assay for the determination of primary amines via fluorescence quenching method. We applied the method to three amine containing antibiotics; amikacin (AMI), gentamicin (GEN) and tobramycin (TOB) that are the members of aminoglycosides. We enhanced the emission signal and lowered the limit of detection by using gold nanoparticles (AuNP).

2. Experimental

2.1. Instrumentation

A Cary Eclipse fluorescence spectrophotometer (Agilent Technologies, California, USA) was used to measure the fluorescence spectra. The UV-Vis spectra were measured with a Shimadzu UV1601 spectrophotometer (Kyoto, Japan). A Mettler Toledo WTW pH meter (Ohio, USA) was used for the pH measurements. The transmission electron microscope (TEM) micrographs were acquired on a FEI Tecnai G2 TEM (Oregon, USA) operated at an acceleration voltage of 120 kV. A Thermo Micro CL21 (New York, USA) and a Nuve NF 200 (Ankara, Turkey) were used for centrifuging.

2.2. Chemicals

TOB (99.8 %), were provided by BILIM Pharmaceuticals (Istanbul, Turkey). Gentamicin sulfate and amikacin sulfate are gift samples from TUM EKIP Pharmaceuticals (Istanbul, Turkey). Gentamicin sulfate and amikacin sulfate were desulfated by the reaction with $BaCl_2$ in acidic medium. Excess amount of $BaCl_2$ were used for precipitation of SO_4^{2-}. All the other chemicals were of analytical grades. The sodium dodecyl sulfate (SDS), HCl, HNO_3, H_3BO_3 $NaNO_2$, $CHCl_3$ were purchased from Merck (Darmstadt, Germany). Lipoic acid, cetyltrimethylammonium bromide (CTAB), 1-ethyl-3-[3-dimethylaminopropyl]carbodiimide hydrochloride (EDC), N-hydroxyisuccinimide (NHS), trichloroacetic acid (TCA), methyl-p-hydroxybenzoate, propyl-p-hydroxybenzoate, glycerine, chlorobutanol, sodium benzoate, lactose, ethanol, $HAuCl_4$, $EuCl_3$, NaOH, H_3PO_4, NaH_2PO_4, NaCl, Na_2CO_3, CH_3COOH, $NaBH_4$ were obtained from Sigma-Aldrich (Steinheim, Germany). Tannic acid, citric acid and ascorbic acid were obtained from Alfa Aesar (Massachusetts, USA). $NaNO_3$, KCl and sodium benzoate were ordered from Riedel de Haen (Seelze, Germany). The water used in the preparation of solutions was ultrapurified by Milli-Q, Millipore system (Darmstadt, Germany).

2.3. Nanoparticle synthesis

2.3.1. Europium nanoparticles

The lipoic acid modified europium nanoparticles were prepared in accordance with the method used by Gao et al.[19] with only slight modifications. 10 mL of tannic acid (0.153 mM) was prepared and stirred vigorously in a water bath (30°C). 1 mL of $EuCl_3$ (10 mM) and 1 mL of SDS (10^{-5} M), which prevents aggregation of nanoparticles, were added while stirring. 10 mM lipoic acid was prepared in ethanol and 0.4 mL was added to the tannic acid solution. After 30 min of stirring, the solution was cooled to 25 °C and diluted to 50 mL with ultrapure water.

2.3.2. Gold nanoparticles

Jana et al.[20] described the preparation of gold nanoparticles of sizes ranging from 5 to 40 nm. In this method, 3.5 ± 0.7 nm gold seed solution and a growth solution were prepared. Through seed-growth control, the size and shape of gold nanoparticle was adjusted.

For the gold seed, 20 mL solution of 0.25 mM $HAuCl_4$ and 0.25 mM trisodium citrate was prepared. While stirring this solution, 0.6 mL of ice-cold and freshly prepared 0.1 M $NaBH_4$ was added. The color of the solution turned pink from the formation of particles. After 2 h this solution was used as the seed.

For the growth solution, 6 g of CTAB was added onto the 200 mL solution of 0.25 mM $HAuCl_4$ and heated until the color of solution turned orange. Then the solution was cooled to room temperature before use.

By changing the volume of seed and growth solutions we prepared spherical and rod shaped nanoparticles of different sizes; 5.5 nm spherical; 8.0 nm spherical; 17 nm spherical; 37.5 nm spherical and 17-200 nm in axis rod.

2.3.3. Characterization

The characterization of EuNP and AuNP was conducted with UV-Vis spectrophotometry and TEM. The UV-Vis spectra were taken against a water blank with a double beam spectrophotometer. EuNP and AuNP were loaded onto carbon formvar coated 200 mesh copper grids and scanned at an accelerating voltage of 120 kV for TEM imaging.

2.4. Method

2.4.1. Activation of the Lipoic Acid

The sensing mechanism was mainly based on the reaction between the carboxylic group of lipoic acid and amine groups of aminoglycosides. However, the reaction of these two groups does not take place at low temperatures since it requires the elimination of water and this occurs at very high temperatures (>473 K)[21] but these high temperatures are generally destructive for samples. For this reason we need to activate lipoic acid with coupling reagents to form an amide bond. We used 0.1 M EDC/NHS solutions for the activation.

2.4.2. Optimization

We optimized the method using the one-factor-at-a-time approach in which the pH, ionic strength, size and shape of enhancer and concentration of enhancer of each experimental factor were optimized separately and independently of the other factors.

The effect of the pH on ΔF was investigated at pH values from 2.0 to 10.0. The Britton-Robinson buffers of pH 2.0-10.0 were prepared with a solution containing 0.04 M H_3BO_3, 0.04 M CH_3COOH and 0.04 M H_3PO_4. Then the pH of buffers was adjusted with 0.2 M NaOH. ΔF values were measured for 30 $\mu g.mL^{-1}$ of each aminoglycosides at each pH.

The effect of ionic strength was investigated with the addition of NaCl from 0 to 2.5 M.

Different size and shape AuNPs were added to enhance the fluorescence. The emissions were recorded just after the addition of AuNP. After determining the best enhancer, the concentration of the enhancer was examined. 0-0.9 mL of AuNP was added to 1.5 mL of EuNP and the samples were diluted with the buffer to a total volume of 3 mL.

2.4.3. Validation

Method validation studies were conducted according to the parameters recommended by the International Conference on Harmonisation (ICH) Q2 (R1) guidelines[22] concerning the validation of analytical procedures for pharmaceuticals consisting of specificity, accuracy, precision, detection and quantitation limits, linearity, range, and robustness. For specificity, excipients in the pharmaceutical formulations and some common ions were assessed. Their tolerance limits, which are concentrations of substances that affect fluorescence signals with a relative error of ±5%, were tabulated. The other parameter linearity was evaluated in terms of correlation coefficients of calibration curves plotted according to the analysis of three sets of AMI, GEN and TOB within the ranges of 0.75-27.5 $\mu g.mL^{-1}$, 0.40-26 $\mu g.mL^{-1}$ and 0.20- 25 $\mu g.mL^{-1}$, respectively. The calibration curves were constructed at ten points by using three sets of aminoglycosides. For accuracy and precision, three sets of 10, 15, and; 20 $\mu g.mL^{-1}$ AMI, GEN and TOB solutions were prepared and analyzed for 3 consecutive days. The parameter precisions were evaluated according to inter-day and intra-day repeatability using relative standard deviations. Biases and percent recoveries were used for accuracy in addition to standard addition experiments that were conducted by adding AMI, GEN and TOB to pharmaceutical at proportion of 50, 75 and 100 % of the pharmaceuticals. The detection and quantitation limits were calculated from equations $3.3\sigma/s$ and $10\sigma/s$ respectively. σ is standard deviation of y-intercept of the calibration curve and s is the slope of the calibration curve. Lastly, the robustness of the method was tested by small but deliberate deviations in the pH. The uncertainty from the pHmeter was 0.1 and the k constant for robustness was taken to be 5. Therefore we tested capacity of the method to remain unaffected in ±0.5 deviations from the optimum pH of the method.

2.4.4. Application

The method was applied to pharmaceuticals and milk samples. 1 g of ointments (Tobrased® containing 0.3% TOB) were dissolved and diluted to 25 mL with a phosphate-citrate buffer (pH 5.0). After 10 minutes of ultrasonication, the samples were stirred on a magnetic stirrer for 20 minutes for the extraction. The samples were filtrated from 0.45 µm pore sized filter papers. 0.1 mL of the filtrates were diluted to 10 mL with a buffer. After the addition of 0.5 mL samples to 1.5 mL of EuNP, 0.4 mL of AuNP was added and the emission spectra were recorded.

Same procedures with TOB were applied to AMI containing pharmaceutical, Dramigel® (5% AMI) and GEN containing pharmaceutical formulation, Belogent® (1 mg GEN/g).

The other matrix; milk samples were spiked with aliquots of AMI, GEN and TOB to achieve final concentrations of 10, 15 and 20 $\mu g.mL^{-1}$. For deproteination and defatting, 1 mL of TCA (1%, w/v) and 0.5 mL of $CHCl_3$ were added to 2 mL of the spiked milk samples. The milk were centrifuged at 4°C and 13000 rpm for 25 minutes after 10 minutes of ultrasonication. Thereafter, supernatants were subjected to another defatting step with 1 M NaOH (0.25 mL) in order to avoid residual fats. The samples were centrifuged at 5000 rpm and the supernatants were filtered using 0.22 mm membrane filters. After these clean-up stages, the samples were neutralized with 1 M HCl and diluted with citrate-phosphate buffer (pH 5.0; 2.5 M NaCl) to final concentrations. 0.5 mL of the samples and 0.4 mL of AuNP were added to 1.5 mL of EuNP and the emission spectra were recorded.

3. Results and discussion

3.1. Nanoparticle Characterization

AuNPs of different shapes and sizes were characterized according to their colors and UV-Vis spectra and the EuNPs were characterized by UV spectrum. 200-800 nm spectra of AuNP (Fig. 1) and 200-400 nm spectrum of EuNP (Fig. 2) were recorded against a water reference in a double beam spectrophotometer. One band of the sphere in UV-Vis spectrum of AuNP was split into two bands in a rod and sphere combination indicating the formation of rods.

Figure 1. UV spectra of gold nanoparticles: a) 5.5 nm spheres b) 8.0 nm spheres c) 17 nm spheres d) 37 nm spheres and 17-200 nm rods

Figure 2. UV spectra of europium nanoparticles a) in absence) in presence of; b) tobramycin c) amikacin sulfate d) gentamicin sulfate e) desulfated amikacin f) desulfated gentamicin

The TEM micrographs show that the EuNPs are in spherical shapes of a size of about 20 nm and the AuNPs consist of spheres and rods (Fig. 3) (~37 nm spheres; ~17-200 nm rods). Emission spectrum of EuNP (λ_{ex} = 280 nm) shows two fluorescence bands at 315 nm and 620 nm and a Rayleigh band at 570 nm (Fig. 4). Surface modification of lipoic acid has nearly no effect on the emission spectrum. The colors, spectra, size and shapes of the nanoparticles obtained in this study are consistent with reference methods of both Gao et al.[19] and Jana et al.[20]. AuNP is stable for several months while EuNP is stable for 6 days at room temperature. UV-Vis absorption spectra of both nanoparticles were stable between 10-60 °C.

Figure 3. TEM micrographs of europium nanoparticles (a-b) and gold nanoparticles (c-d)

Figure 4. Emission spectrum of europium nanoparticles a) before and b) after enhancement with gold nanoparticles (λ_{ex}=280 nm)

3.2. Quenching Type

Addition of aminoglycosides to lipoic acid capped EuNP after NHS/EDC activation resulted in fluorescence quenching (Fig. 5). We speculate that the fluorescence quenching of EuNP stems from the binding of amine groups to the particles through carboxyl group of the linker; lipoic acid. Therefore, the quenching type is supposed to be mainly static quenching with formation of a non-fluorescent product. We proved this with spectrophotometric measurements and the Stern-Volmer equations derived from the emission spectrums taken different temperatures.

Figure 5. Fluorescence quenching of europium nanoparticles in the presence of tobramycin (0-25 μg.mL^{-1})

For the quenching type analysis, we firstly measured UV absorption spectrums of lipoic acid modified EuNP in the absence and presence of TOB (Fig. 2). We deduce that great difference in UV absorption spectrums of nanoparticles shows a ground-state complex formation between the nanoparticles and aminoglycosides. If quenching arose from dynamic quenching, the UV spectrum of fluorophore would not change in the presence of a quencher since in dynamic quenching, only the excited state fluorescent molecule interacted with the quencher. On the contrary, in static quenching, the quencher forms complex with the ground state fluorescent molecule, therefore it affects absorption spectrum of the fluorescent substance[23]. Although TOB has no UV chromophore group, the addition of TOB to lipoic acid capped EuNP obviously changed the UV spectrum. However in case of sulfate form of AMI and GEN, no change in UV spectrum of EuNP was observed (Fig 2). Complex formations for AMI and GEN were yet measured after desulfation of them. This is probably stem from steric hindrance of sulfate form of aminoglycosides.Therefore AMI and GEN were desulfated before all experiments.

The Stern-Volmer curves were plotted from equation:

$$\frac{F_0}{F} = 1 + K_{sv}[C]$$

The F_0 and F fluorescence of EuNP in the absence and presence of aminoglycosides, K_{sv} is the Stern-Volmer quenching constant and [C] is the concentration of aminoglycosides. The slope of F_0/F vs [C] gives K_{sv} while intercept is equal to 1. The linearity of this curve shows whether the quenching type is a single class or not. If it is linear, then quenching type is only static or dynamic. When there is a deviation from linearity, then the quenching is a combination of both types. The curves for the aminoglycosides quenching are linear (Fig. 6) hence the quenching is a single class. We conducted the quenching experiments at different temperatures (288, 298 and 308 K) to determine this class. The slopes (K_{sv}) were decreased by increasing the temperature (Fig. 6). In static quenching, the increase in temperatures induces the dissociation of weakly bound complexes that will result in a decrease of the quenching constant. In the dynamic quenching, it increases collisions and the quenching constant.[1] Table 1 shows K_{sv} values at different temperatures. This data reveals that the quenching results from a complex formation between lipoic acid capped EuNP and aminoglycosides.

Figure 6. The Stern-Volmer curves at different temperatures

Table 1. Stern-Volmer constants

	K_{sv}		
	288 K	298 K	308 K
AMI	18342	16657	15133
GEN	14829	13930	13850
TOB	24986	21278	20939

3.3. Binding parameters

We demonstrated complex formation between primary amines and lipoic acid capped EuNP by quenching type experiments. Binding constant and number of binding sites were also indicated by the equation:

$$\log \frac{(F_0-F)}{F} = K_b + n \log[C]$$

K_b is the binding constant and n is the number of binding sites in this equation. Slope and intercept of the log $(F_0\text{-}F)/F$ vs log[TOB] graph gives the number of binding sites and binding constant respectively (Table 2).

Thermodynamic parameters; enthalpy change (ΔH^o), entropy change (ΔS^o) and free energy change (ΔG^o); were also calculated (Table 2). We used van't Hoff plot for calculations:

$$\ln K = -\frac{\Delta H^o}{RT} + \frac{\Delta S^o}{R}$$

$-\Delta H^o/R$ and $\Delta S^o/R$ are the slope and the intercept of lnK vs 1/T curve respectively. ΔG^o is calculated from the following equation:

$$\Delta G^o = \Delta H^o - T\Delta S^o$$

Results revealed that covalent bond formation between carboxylic group of lipoic acid and primary amines is an exothermic process and occurs spontaneously.

3.4. Method Optimization

3.4.1. pH

The variations in the pH value changes reaction yield between the lipoic acid on the surface of EuNP and the aminoglycosides. The pH of the solution was controlled by the Britton-Robinson buffers within the range of 2.0-10.0 pH. The ΔF values are generally higher in an acidic medium than the basic medium and at the highest values at pH 5. This arises from the higher fluorescence characteristic of the lipoic acid capped EuNP at acidic medium than that at the basic medium. The other reason for the high ΔF at pH 5.0 is that activation of the carboxyl groups by EDC/NHS reagents is most efficient at pH 4.5-7.2.

3.4.2. Ionic strength

In the quenching experiments, it is significant to maintain a constant ionic strength[1]. Therefore, we adjusted NaCl concentration such a high value of 2.5 M. In this way the addition of any reagents in the experiment have a negligible effect on the ionic strength.

3.4.3. Size and concentration of AuNP

In this study, we synthesized different types of AuNP and observed their effects on the fluorescence signals. The optical properties of AuNP are sensitive to the size, shape, concentration of the nanoparticles and refractive index near to the nanoparticles.[24] We observed the optical properties of AuNP in terms of their colors and spectrums. The color of the AuNP turned from wine red to brown by increasing the size of nanoparticles. The spectrums of different sizes and shapes of AuNP can be seen in Figure 1. The highest enhancement factor was observed for mix of spheres (37 nm) and rods (17x200 nm).

T (K)	K_b ($x10^4$ L mol^{-1}) ± SD	n	ΔH^o (kJ mol^{-1})	ΔS^o (J mol^{-1} K^{-1})	ΔG^o (kJ mol^{-1})
288	5.58 ± 0.21	1.12	-28.2	11.1	-31.4
298	2.72 ± 0.09	1.20			-31.5
308	2.61 ± 0.11	1.15			-31.6

Table 2. Binding constants, binding sites and thermodynamic parameters

The fluorescence was enhanced by increasing the concentration of AuNP. However, at high concentrations of AuNP fluorescence enhancement was decreased. This is probably because of the self-interaction between plasmon electrons of AuNPs. At higher concentrations of AuNP, the electric field that is responsible for signal enhancement is decreased by this phenomenon. Optimum signal enhancement is achieved at 0.4 mL of AuNP ($0.42x10^{-4}$ M Au) which is considered to give the maximum electric field for the fluorophore groups in signal enhancement.

After the MEF studies, fluorescence of EuNP was enhanced (Fig. 4) and the detection limit was lowered by 2.9 times. In a previously reported lanthanide ion probe spectroscopy method (LIPS)[18], AMI, GEN and TOB was determined in a range of 10-70 μg.mL^{-1} by using europium–aminoglycosides complex formation. By utilizing nanoparticle form of europium, we improved sensitivity of the assay to about 50 times greater than the LIPS method. This proves that the use of nanoparticles of a substance can greatly improve the sensitivity of an analytical technique.

3.5. Method Validation

The specificity of the method was investigated to determine tolerance limits of excipients in the pharmaceuticals, milk sugar, and the common ions (Table 3). These results demonstrate the methods specific for primary amines in the presence of possible interferrants of selected samples.

Table 3. Tolerance limits

Substances	Tolerance limits (μg.mL^{-1})
Methyl-p-hydroxybenzoate	>1522
Propyl-p-hydroxibenzoate	>400
Benzoate	104
Chlorobutanol	>17746
Betamethasone dipropionate	> 130
Lactose	>34230
Glycerin	126000
Nitrite	445
Nitrate	1061
Potassium	>7460
Carbonate	59
Acetate	727
Sodium	>10000
Chloride	>10000

The method is linear in the range of 0.40-27.5 μg.mL^{-1}, 0.25-26 μg.mL^{-1}, 0.20 – 25 μg.mL^{-1} with correlation coefficients of 0.9965, 0.9966 and 0.9969 for AMI, GEN and TOB respectively. The percent recoveries and relative standard deviations of inter-day and intra-day analysis show good accuracy and precision (Table 4). The standard addition method is also a complementary method for achieving accuracy in the analysis of the pharmaceutical preparations.

		Intra-day		Inter-day	
	Conc. (μg.mL^{-1})	Recovery (%)	RSD (%)	Recovery (%)	RSD (%)
AMI	10	102.64	1.00	101.10	1.84
	15	99.43	0.87	99.83	1.07
	20	100.03	0.36	99.33	1.06
GEN	10	97.43	2.26	97.82	1.46
	15	98.52	1.77	99.53	1.30
	20	102.76	0.92	102.59	1.00
TOB	10	101.2	3.64	100.9	2.34
	15	96.8	0.82	99.8	3.88
	20	103.1	1.12	102.7	2.35

Table 4. A ccuracy and precision results

The detection and quantitation limits calculated from the slope and standard deviations of the calibration curve are: 223 ng.mL^{-1} and 746 ng.mL^{-1} for AMI, 91 ng.mL^{-1} and 304 ng.mL^{-1} for GEN, and 59.7 ng.mL^{-1} and 199 ng.mL^{-1} for TOB; respectively. Sensitivity of the assay is higher than classical spectroscopic, voltammetric and CE-UV techniques while it is still lower than the complicated ones like LC-MS/MS, CE-LIF and voltammetry with modified electrodes (Table 5).

The method was also tested against the deviation in pH. We found that the method remained unaffected by small deviations in pH.

MEF studies are generally conducted on a surface platform, because the enhancement factor can reach several thousand. MEF can also be useful in solution-based platform but generally the signal enhancement factor is much less (3-5 fold) than the surface platform.[25] On the other hand, the solution-based platform is easier and has higher reproducibility than the surface studies. Good validation results support applicability and reproducibility of this solution-based MEF method.

Table 5. Comparison of sensitivity the assay with previous methods

Methods	Sample	Detection Limits
LC-MS/MS[9]	AMI	8 ng.mL^{-1}
	GEN	11 ng.mL^{-1}
	TOB	10 ng.mL^{-1}
LC-MS[10]	GEN	13 ng.mL^{-1}
CE-LIF[11]	AMI	10 ng.mL^{-1}
	TOB	20 ng.mL^{-1}
CE-UV[12]	AMI	200 µg.mL^{-1}
	TOB	80 µg.mL^{-1}
Voltammetry[13]	AMI	300 ng.mL^{-1}
Voltammetry[14]	TOB	0.65 ng.mL^{-1}
Spectrophotometry[15]	AMI	3000 ng.mL^{-1}
	GEN	2000 ng.mL^{-1}
	TOB	1000 ng.mL^{-1}
Spectrofluorimetry[17]	GEN	112 ng.mL^{-1}
Our method	AMI	223 ng.mL^{-1}
	GEN	91 ng.mL^{-1}
	TOB	60 ng.mL^{-1}

3.6. Application

The spiked milk samples were analyzed and acceptable results were obtained (Table 6). Analysis of antibiotic residues in milk is usually performed in two steps[26]. In the first step detection and identification of the antibiotic is conducted by microbial, enzymatic or receptor-based methods. In the second step quantification is carried out. Our method is suitable for the second step.

The analysis of the pharmaceutical samples resulted in a very close agreement with labeled values (Table 7). We also compared these results with our previous method[16] using a t and F test.

Table 6. Analysis of milk samples

	Spiked (µg.mL^{-1})	Found (µg.mL^{-1})	Recovery (%)	RSD (%)
AMI	10	10.48	104.80	9.23
	15	14.47	96.45	2.34
	20	22.58	112.89	3.80
GEN	10	11.27	112.72	3.98
	15	16.92	112.82	1.04
	20	20.81	104.05	0.90
TOB	10	10.81	108.11	6.18
	15	14.79	98.63	2.44
	20	22.14	110.70	3.08

Table 7. Analysis of pharmaceuticals

	Found	Recovery (%)	RSD (%)	t calculated	F calculated
Dramigel® (5% AMI)	5.10 %	101.94	1.74	1.67	2.01
Belogent® (1 mg GEN)	1.00 mg	99.62	1.60	2.09	1.28
Tobrased® (0.3% TOB)	0.31 %	101.92	2.90	1.63	1.04

SD:Standard deviation tabulated t=2.23 for d.f.=10 and F = 5.05 for d.f.: 5-5

4. Conclusions

We developed a metal enhanced fluorescence assay for the determination of primary amines. The method in which we used AuNP and EuNP was applied to aminoglycosides in pharmaceuticial preparations and milk samples. Synthesis of EuNP does not require toxic chemicals like in the synthesis of quantum dots and the process is cheap, easy and rapid. Reaction of primary amines and lipoic acid on the surface of EuNP resulted fluorescence quenching. The fluorescence quenching was found to be mainly caused by static quenching from the Stern-Volmer constants and the UV spectra of ground-state interactions. The sensitivity of the method was enhanced by AuNP and the detection limits was lowered. The method was optimized in the factors of pH, ionic strength, shape and size of AuNP and concentration of AuNP. The method was validated according to the ICH guidelines for analytical validation of pharmaceuticals. The method is selective against excipients of pharmaceutical formulations and other possible interferants of milk. We successfully applied this low-cost and simple method to pharmaceutical and milk samples. For further studies, we are working on transferring the solution-based assay to surface platform for enhancing the sensitivity and selectivity.

Acknowledgements

Financial support from Ankara University Scientific Research Funds (14B0237001) is gratefully acknowledged.

Notes and references

1 J.R. Lakowicz, *Principles of Fluorescence Spectroscopy*, 3rd ed., Springer, New York, 2006.
2 H. Harma, T. Soukka and T. Lovgren, *Clin. Chem. (Washington, DC, U. S.)*, 2001, **47**, 561-568.
3 D. L. Feldheim and C. A. Foss, Jr*., Metal nanoparticles*, Marcel Dekker, Inc., 2002, pp. 1-15.
4 J. P. Anderson, M. Griffiths, J. G. Williams, D. L. Grone, D. L. Steffens and L. M. Middendorf, in *Metal Enhanced Fluorescence*, ed. C. D. Geddes, John Wiley & Sons, Inc., 2010, pp. 119-137.
5 A. M. Lovering, D. S. Reeves, in *Antibiotic and Chemotherapy*, ed.R. G. Finch, D. Greenwood, S. R. Norrby, R. J. Whitley, Elsevier, Amsterdam, 9th edn., 2010, ch. 12, pp 145-170.
6 M. G. Papich and J. E. Riviere, in *Veterinary Pharmacology &Therapeutics*, ed. J. E. Riviere and M. G. Papich, Blackwell Publishing Professional, 2009, pp. 915-944.
7 H. C. Neu and C. L. Bendush, *J Infect Dis*, 1976, **134 Suppl**, S206-218.
8 A. M. Stolker and U. A. T. Brinkman, *J. Chromatogr. A*, 2005, **1067**, 15-53.
9 Y. Tao, D. Chen, H. Yu, L. Huang, Z. Liu, X. Cao, C. Yan, Y. Pan, Z. Liu and Z. Yuan, *Food Chem.*, 2012, **135**, 676-683.
10 S. B. Turnipseed, S. B. Clark, C. M. Karbiwnyk, W. C. Andersen, K. E. Miller and M. R. Madson, *J. Chromatogr. B: Anal. Technol. Biomed. Life Sci.*, 2009, **877**, 1487-1493.
11 C.-Z. Yu, Y.-Z. He, G.-N. Fu, H.-Y. Xie and W.-E. Gan, *J. Chromatogr. B: Anal. Technol. Biomed. Life Sci.*, 2009, 877, 333-338.
12 H.-H. Yeh, S.-J. Lin, J.-Y. Ko, C.-A. Chou and S.-H. Chen, *Electrophoresis*, 2005, **26**, 947-953.
13 X. L. Wang, Z. Y. Yu and K. Jiao, *Chin. Chem. Lett.*, 2007, 18, 94-96.
14 V. K. Gupta, M. L. Yola, N. Ozaltin, N. Atar, Z. Ustundag and L. Uzun, *Electrochim. Acta*, 2013, **112**, 37-43.
15 M. A. Omar, D. M. Nagy, M. A. Hammad and A. A. Aly, *J. Appl. Pharm. Sci.*, 2013, **3**, 151-161, 111 pp
16 M. G. Caglayan and F. Onur, *Spectrosc. Lett.,* 2014, **47**, 771-780.
17 A. A. Al-Majed, F. Belal, M. A. Abounassif and N. Y. Khalil, *Mikrochim. Acta*, 2003, **141**, 1-6.
18 M. Rizk, Y. El-Shabrawy, N. A. Zakhari, S. S. Toubar and L. A. Carreira, *Talanta*, 1995, **42**, 1849-1856S.
19 X. B. Gao, J. Yu, N. Li, H. Y. Yin and J. H. Yang, *Chin. Chem. Lett.,* 2007, **18**, 1289-1292.
20 N. R. Jana, L. Gearheart and C. J. Murphy, *Langmuir*, 2001, **17**, 6782-6786.
21 E. Valeur and M. Bradley, *Chem. Soc. Rev.,* 2009, **38**, 606-631.
22 ICH Harmonized Tripartite Guideline, International Conference on Harmonization of Technical Requirements for registration of Pharmaceuticals for Human Use, Validation of Analytical Procedure:Text and Methodology Q2(R1) (1996) International Conference on Harmonization, Geneva, Switzerland.
23 A. Gong, X. Zhu, Y. Hu and S. Yu, *Talanta*, 2007, **73**, 668-673.
24 K. Aslan, J. R. Lakowicz, H. Szmacinski and C. D. Geddes*, J. Fluoresc.,* 2004, **14**, 677-679.
25 K. Aslan and C. D. Geddes, in *Metal Enhanced Fluorescence*, ed. C. D. Geddes, John Wiley & Sons, Inc. 2010, pp. 1-23.
26 International dairy Federation (IDF), 1995, Residues of antimicrobial drugs and other inhibitors in milk. Proceedings of the IDF – symposium in Kiel, Germany, August 28-31, Brussels, Belgium.

FIGURES

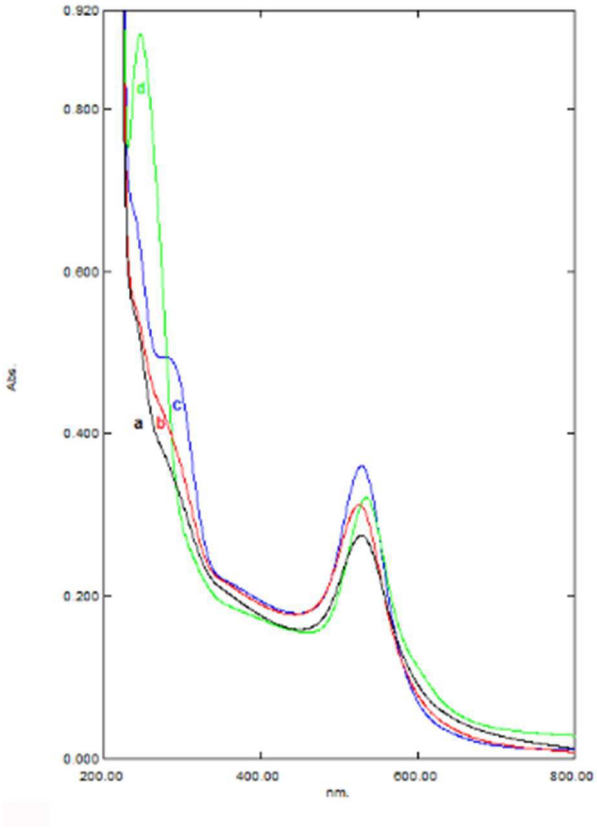

Figure 1. UV spectra of gold nanoparticles: a) 5.5 nm spheres b) 8.0 nm spheres c) 17 nm spheres d) 37 nm spheres and 17-200 nm rods

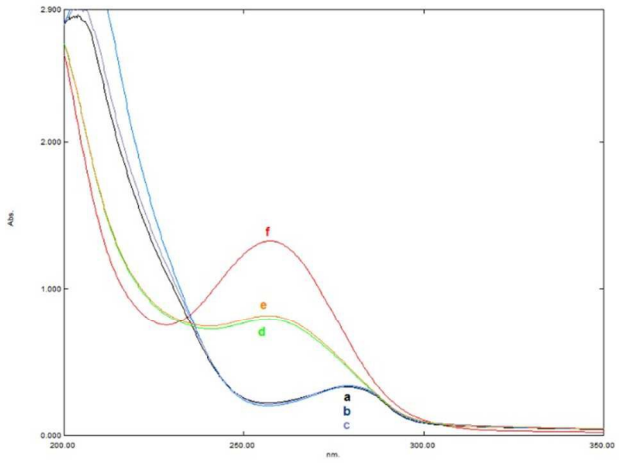

Figure 2. UV spectra of europium nanoparticles a) in absence) in presence of; b) tobramycin c) amikacin sulfate d) gentamicin sulfate e) desulfated amikacin f) desulfated gentamicin

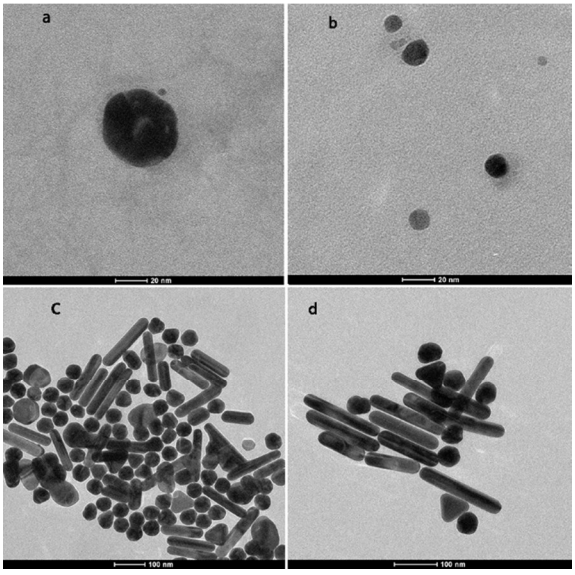

Figure 3. TEM micrographs of europium nanoparticles (a-b) and gold nanoparticles (c-d)

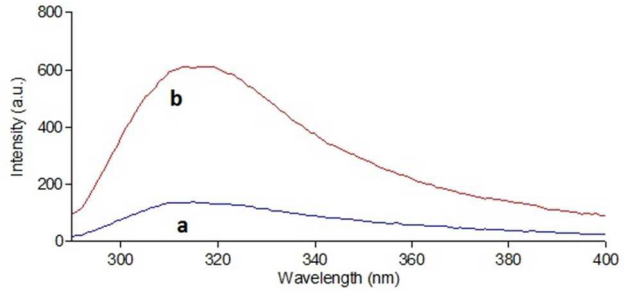

Figure 4. Emission spectrum of europium nanoparticles a) before and b) after enhancement with gold nanoparticles (λ_{ex}=280 nm)

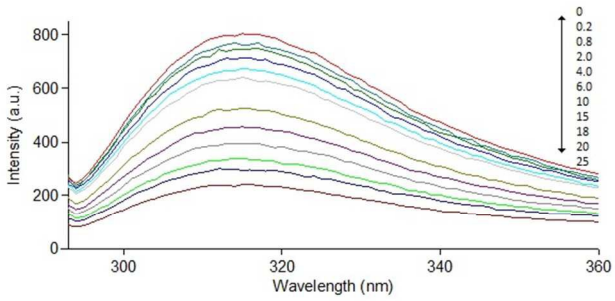

Figure 5. Fluorescence quenching of europium nanoparticles in the presence of tobramycin (0-25 µg.mL^{-1})

Figure 6. The Stern-Volmer curves at different temperatures

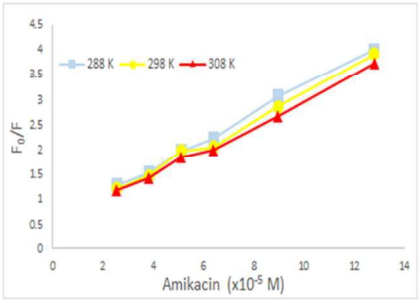

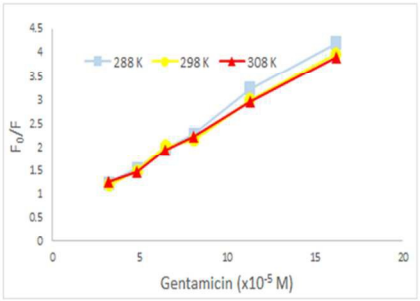

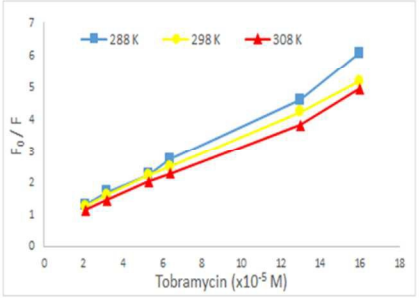

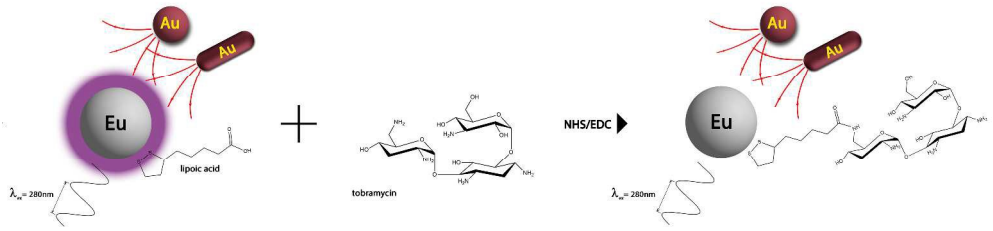

817x204mm (300 x 300 DPI)